

Case Study

Systemic Coronaviral Disease in 5 Ferrets

Christopher R Autieri,¹ Cassandra L Miller,^{1,4} Kathleen E Scott,¹ Alexandra Kilgore,² Victoria A Papscoe,² Michael M Garner,³ Jennifer L Haupt,¹ Vasudevan Bakthavatchalu,¹ Sureshkumar Muthupalani,¹ and James G Fox^{1,*}

The prevalence of reported systemic coronaviral disease in ferrets (*Mustela putorius furo*), which resembles the dry form of feline infectious peritonitis, has been increasing in the literature since its initial diagnosis and characterization approximately 10 y ago. Here we describe the clinical signs, pathologic findings, and diagnosis by immunohistochemistry using an FIPV3-70 monoclonal antibody of systemic coronaviral disease in 5 ferrets, 2 of which were strictly laboratory-housed; the remaining 3 were referred from veterinary private practices. This case report illustrates the importance of considering FRSCV infection as a differential diagnosis in young, debilitated ferrets with abdominal masses and other supporting clinical signs.

Abbreviations: FCoV, feline coronavirus; FIPV, feline infectious peritonitis virus; FRSCV, ferret systemic coronavirus

Coronaviruses are enveloped, pleomorphic, positive-strand RNA viruses with a diameter of 60 to 220 nm and classified under the genus *Coronavirus* within the family Coronaviridae, order Nidovirales.⁹ The viral particles typically develop in the cytoplasm of affected epithelial cells and macrophages inside vacuoles and form characteristic radiating peplomer spikes on the surface of the envelope, a diagnostic feature when imaged by electron microscopy. In domestic ferrets (*Mustela putorius furo*), coronaviruses have been implicated as the cause of 2 distinct clinical conditions, namely epizootic catarrhal enteritis (caused by ferret enteric coronavirus) and ferret systemic coronavirus (FRSCV)-associated disease.¹ Epizootic catarrhal enteritis was first observed in Spring 1993 on the East coast of the United States, and a detailed description of the disease and its association with coronavirus was first published in 2000.¹¹ Epizootic catarrhal enteritis affects all age groups of ferrets but is most severe in aged animals, whereas FRSCV disease, which was first documented in Spain in 2006, is now being recognized sporadically in multiple locations and affects young animals (mean age, 11 mo; range, 2 to 36 mo).²

Epizootic catarrhal enteritis is primarily an enteric disease, with lesions consistent with intestinal coronaviral infection and including vacuolar degeneration and necrosis of villous enterocytes, villous atrophy, blunting and fusion, and lymphocytic enteritis.¹ In contrast, the clinical and pathologic presentation of FRSCV infection resembles the dry form of feline infectious peritonitis virus (FIPV)-induced disease,⁵ which develops in cats as the result of an uncommon (1% to 3%) de novo mutation in the ubiquitous feline coronavirus (FCoV).⁴ FIPV-associated disease can manifest in cats as a dry, noneffusive form or a wet, effusive form, which is

characterized by the accumulation of fluid within the peritoneal or thoracic cavities, depending on the host immune response.

The noneffusive forms of feline infectious peritonitis and FRSCV cause pyogranulomatous to granulomatous lesions in multiple organs. Histologically, pyogranulomatous inflammation appears as a central area of necrotic cellular debris and degenerative neutrophils surrounded by epithelioid macrophages with occasional multinucleated giant cells and layers of lymphoplasmacytic infiltrates with a variable degree of fibrosis.^{2,9} Because this form of inflammation displays a vasculocentric distribution, vasculitis affecting small arterioles and venules is also a common finding.^{2,9} Organs affected during noneffusive FIPV and FRSCV infections include the spleen, mesenteric lymph nodes, intestines, kidneys, and brain, in contrast to ferrets with ECE and the majority of symptomatic cats positive for FCoV, in which lesions are typically limited to the gastrointestinal tract. Common clinical signs of FRSCV include anorexia, weight loss, diarrhea and a palpable intraabdominal mass. Less frequent findings include hindlimb paresis and CNS dysfunction. Immunoreactivity with FCoV antigen on paraffin sections or serum samples from suspected cases of FRSCV has been demonstrated in all cases of ferrets with concurrent granulomas.^{2,6,7} As expected with pyogranulomatous inflammation and concurrent vasculitis, positive staining is seen within the surrounding macrophages and vascular endothelium. In this report, we describe 5 cases of ferrets with the clinical signs, progression, and pathologic hallmarks characteristic of FRSCV disease and confirm infection through immunohistochemistry using an FIPV3-70 monoclonal antibody (Custom Monoclonals International, West Sacramento, CA).

Case Reports

Case 1. A 15-mo-old, male, laboratory-housed fitch ferret presented for necropsy after a 1-wk history of greenish diarrhea progressing to hematochezia. The ferret was singly housed in a modified rabbit cage within a cubicle containing several other singly housed ferrets at the Massachusetts Institute of Technology,

Received: 20 Mar 2015. Revision requested: 29 Apr 2015. Accepted: 14 Jun 2015.

¹Division of Comparative Medicine, Massachusetts Institute of Technology, Cambridge, Massachusetts; ²Littleton Animal Hospital, Littleton, Massachusetts; and ³Northwest ZooPath, Monroe, Washington.

⁴Current address: SNBL USA, Everett, Washington.

*Corresponding author. Email: jgfox@mit.edu

an AAALAC-accredited facility. This ferret was the offspring of a sire and dam obtained from Marshall Farms (North Rose, NY) and did not undergo any experimental manipulations. No other ferrets displayed any signs of clinical illness. The ferret exhibited rapid progression of weakness, lethargy, inappetence, and eventual anorexia, with a 200-g decrease in body weight over a 1-wk period. Serum chemistry findings included hyperglycemia (240 mg/dL; reference range, 80 to 120 mg/dL), elevated liver enzymes (ALT, 328 IU/L [reference, 10 to 280 IU/L]; AST, 670 IU/L [reference, 50 to 280 IU/L], and GGT, 16 IU/L [reference, less than 10 IU/L]), elevated creatine kinase (5152 IU/L; reference, 98 to 564 IU/L), panhypoproteinemia (albumin, 1.1 g/dL [reference 2.4 to 4.5 g/dL]; globulin, 2.5 g/dL [reference 2.9 to 4.9 g/dL]), and hypocalcemia (7.1 mg/dL; reference, 7.7 to 11 mg/dL). Supportive care including subcutaneous fluids, broad-spectrum antibiotics, and supplemental feedings was ineffective, and the ferret was euthanized for humane and diagnostic purposes.

Postmortem gross observations included an empty gastrointestinal tract with a focal gastric ulcer; hyperemia and segmental thickening of the jejunum, ileum, and rectum; enlarged nodular mesenteric lymph nodes (Figure 1 A); splenomegaly with multiple tan nodular masses; and left ventricular dilatation. Histologically, there was multisystemic granulomatous inflammation involving the mesenteric lymph nodes, peritoneum and mesentery, spleen, and mucosal-associated lymphoid tissue of the small and large intestines (Figure 1 B through D). In addition, small numbers of epithelioid macrophages mixed with lymphocytes and plasma cells were present in a few perivascular foci within the meninges of the brain (Figure 1 E). Ziehl–Neelsen acid-fast and periodic acid–Schiff staining revealed no mycobacteria or fungal organisms, respectively, in the lesions. Immunohistochemical staining for feline coronavirus antibody performed at the Washington State University Animal Disease Diagnostic Lab (Figure 1 F) revealed mild to moderate multifocal cytoplasmic positivity within macrophages in the central core of granulomas of the mesenteric lymph node. Subsequent inhouse immunohistochemistry using FIPV3-70 monoclonal antibody (Figure 1 G) showed similar positive immunoreactivity. On the basis of these findings, a diagnosis of a systemic coronaviral disease was made. Selected archival lymph node specimens from 10 ferrets that had been housed at the institution over the previous 20 y were screened by using FIPV3-70 monoclonal antibody and did not identify any animals with a positive reaction. These cases comprised both healthy ferrets and those diagnosed with gastritis or lymphoma.

Case 2. A 7-mo-old female ferret presented to a veterinary private practice with a 3-wk history of decreased appetite and bruxism. The ferret had contact with 2 other ferrets as well as multiple other species, including cats, dogs, ducks, and guinea pigs. None of these other animals displayed any signs of morbidity. Physical examination revealed poor body condition and a palpable abdominal mass. A serum chemistry panel revealed hypoalbuminemia, and laparoscopy revealed nodular, white foci on the majority of abdominal organs and mesentery and a 3-cm mass at the root of the mesentery. The ferret was euthanized, and tissues in formalin were submitted for further diagnostic evaluation. Grossly, the spleen was enlarged, with multiple, raised, coalescing tan nodules extending from the surface into the parenchyma. The liver exhibited a 3-cm irregular, nodular, tan mass along the lateral edge of the left lobe, with a few small, tan foci on all other

lobes. A 2-mm, pale, yellow nodule was present in the lung. The mesentery contained multiple, tan to yellow nodules throughout and was thickened along vessels. Gastric and mesenteric lymph nodes were enlarged and adherent to adjacent tissues. Histologically, all tissues revealed evidence of moderate to severe multifocal to coalescing granulomatous and lymphocytic inflammation, which was most severe in the lymph nodes (Figure 2 A), liver, mesenteric vessels, and small intestine. The mesenteric lymph nodes, spleen, liver, small intestine, kidneys, and adrenal gland were negative for acid-fast organisms, whereas immunohistochemistry using FIPV3-70 monoclonal antibody was strongly positive in the cytoplasm of macrophages within granulomas of multiple organs, including the mesenteric lymph node, mesenteric vessels, and small intestine (Figure 2 B through D).

Case 3. A 6-mo-old, castrated male ferret was initially diagnosed with ferret granulomatous coronavirus-associated disease at a veterinary private practice. Clinical findings at that time included diarrhea, lethargy, anorexia, and a palpable abdominal mass. CBC and serum chemistry analysis performed at an external diagnostic laboratory (Antech Diagnostics, Ballston Lake, NY) revealed anemia (PCV, 23%; reference, 43 to 55), leukocytosis ($14 \times 10^3/\mu\text{L}$; reference, 2.5 to $8.0 \times 10^3/\mu\text{L}$) with 89% lymphocytes, mild hypoalbuminemia (1.6 g/dL; reference, 2.6 to 3.8 g/dL) and mild hyperglobulinemia (3.6 g/dL; reference, 1.8 to 3.1 g/dL). Abdominal radiographs (Figure 3 A and B) revealed a poorly defined area of increased opacity in the midabdomen apparent on the lateral but not ventrodorsal views. An exploratory laparotomy revealed a 4-cm white, nodular, highly vascular mass at the mesenteric root. The mass was judged to be surgically nonresectable. Biopsy of the mass revealed severe pyogranulomatous inflammation with reactive fibrosis and multifocal regions of necrosis and fibrin deposition. Neoplastic cells and infectious agents were not identified. Immunohistochemical staining at a diagnostic referral laboratory confirmed the presence of coronavirus antigen in inflammatory foci.

The ferret was maintained with at-home supportive care, including intermittent antimicrobial therapy to treat diarrhea, sucralfate, potassium supplements, and syringe-feeding of high-calorie, highly palatable soft foods. An abdominal ultrasound 5 wk after initial diagnosis revealed a multilobular midabdominal mass 2.7 cm in diameter (Figure 3 C). Serial bloodwork revealed progressive hypoalbuminemia, hyperglobulinemia, hypokalemia, and intermittent anemia and neutrophilic leukocytosis. Oral prednisone (1 mg/kg daily) was prescribed approximately 2 mo after initial diagnosis. After continued decline, the ferret was euthanized at 18 mo of age and presented for gross and histopathologic examination.

Gross postmortem findings included multiple, firm, tan, 1- to 5-mm nodules throughout the mesentery (Figure 3 D), bilateral pale cortical pitting lesions on the kidneys (Figure 3 E), multiple, coalescing, raised white nodules in the lungs with complete consolidation of the accessory lobe (Figure 3 F), and splenomegaly with pinpoint, pitted lesions (Figure 3 G). Histologically, there was multisystemic granulomatous to pyogranulomatous inflammation either in the form of discrete or coalescing foci prominently involving the mesenteric nodes (Figure 4 A), lungs, pancreas, intestinal serosa, and peritoneum. The lungs had multifocal consolidation with severe pulmonary edema, necrosis, and suppurative bacterial pneumonia, attributed to aspiration associated with syringe feeding (Figure 4 B and C). The kidneys

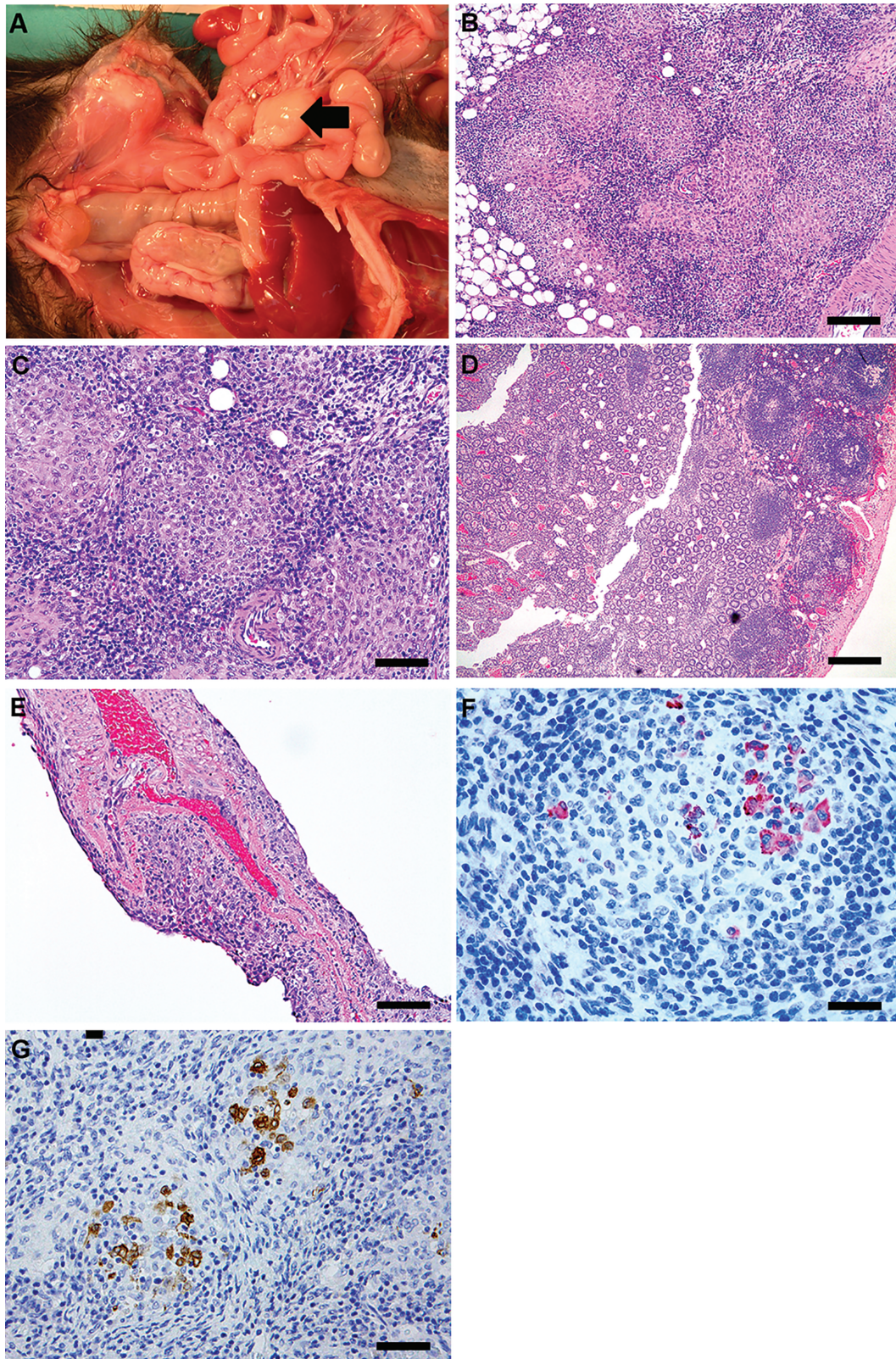


Figure 1. Case 1. (A) Enlarged mesenteric lymph node (MLN) apparent on necropsy. (B) Enlarged MLN displaying effacement of nodal architecture by multifocal to coalescing, discrete nodular foci of epithelioid macrophages (bar, 100 μ M). (C) Higher magnification of MLN in panel B, showing highly cellular structure of the granulomas comprising epithelioid macrophages surrounded by lymphocytes and few fibroblasts (bar, 50 μ M). (D) Ileum at low magnification displaying mucosal congestion, venous ectasia, and scattered to discrete inflammatory aggregates composed of lymphocytes, plasma cells, and few neutrophils (bar, 500 μ M). (E) The leptomeninges of the cerebral cortex are expanded by perivascular aggregates of lymphocytes

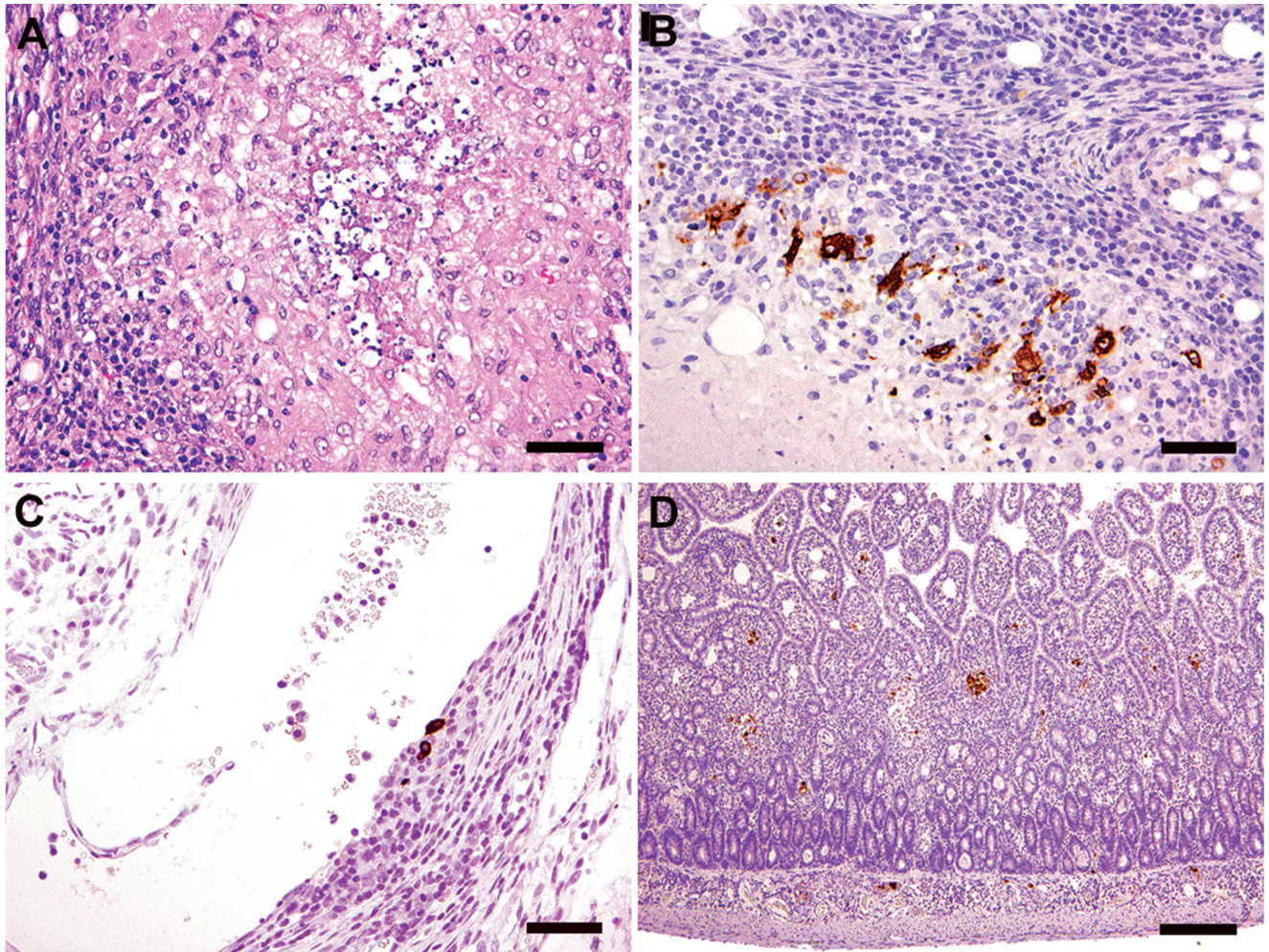


Figure 2. Case 2. (A) Mesenteric lymph node displaying severe multifocal to coalescing necrogranulomatous lymphadenitis (hematoxylin and eosin stain; bar, 50 μ M). Immunohistochemistry showed positive (brown) staining for feline coronavirus (FIPV3-70) monoclonal antibody in (B) a mesenteric lymph node (bar, 50 μ M), (C) a mesenteric vessel (bar, 50 μ M), and (D) the small intestine (bar, 200 μ M).

had prominent cortical lymphoplasmacytic interstitial nephritis and chronic sclerotic glomerulopathy (Figure 4 D). Periodic acid–Schiff and Gomori methenamine silver stains of the lung tissue were negative for fungal organisms. A Ziehl–Neelsen acid fast stain of lung, mesenteric lymph node, stomach and intestine was negative for acid-fast bacilli. In the kidneys, FIPV3-70 positive immunoreactivity was noted within macrophages scattered among the lymphoplasmacytic inflammatory aggregates in the interstitium (Figure 4 E). Ultrastructurally, coronavirus-like particles within macrophages, either inside cytoplasmic vacuoles or free in the cytosol were identified via electron microscopy (Figure 4 F).

Case 4. A 10-mo-old female ferret presented to a private veterinary practice with a history of weight loss, lethargy, and green mucoid diarrhea of unknown duration. The ferret was in contact with 8 other ferrets in the household, one of which displayed similar, but less severe, clinical signs. Physical exam revealed

dehydration, pale mucous membranes, poor body condition, and a 1-cm firm, irregular midabdominal mass. A serum chemistry panel revealed hypoproteinemia and hypoalbuminemia (Antech Diagnostics). After lack of response to supportive care, the ferret was euthanized and a necropsy performed by the referring veterinarian. Gross postmortem findings included a small trichobezoar in the stomach and a firm, irregular, thickened mesenteric root. Formalin-fixed tissues were submitted to a consulting pathologist for further evaluation.

Histologically, foci of pyogranulomatous inflammation and necrosis were present within and around blood vessels and randomly throughout the kidney, liver, intestinal wall, mesenteric root and lymph nodes, and pancreas. Inflammation was predominantly neutrophilic, with fewer mononuclear cells. Within the pancreas and lymph nodes, inflammation was more frequently oriented around accumulations of necrotic cell debris. Acid-fast staining was negative for *Mycobacterium* spp., but immunohistochemistry

and macrophages (bar, 100 μ M). Hematoxylin and eosin stain (B through E). (F) Immunohistochemistry (feline coronavirus antibody) of MLN. Macrophages within the central cores of granulomas exhibit mild to moderate multifocal cytoplasmic positivity (bar, 50 μ M). (G) Immunohistochemistry of MLN, with positive staining for feline coronavirus (FIPV3-70) monoclonal antibody. This antibody is crossreactive for type 1 coronaviruses and is used for definitive diagnosis (bar, 50 μ M).

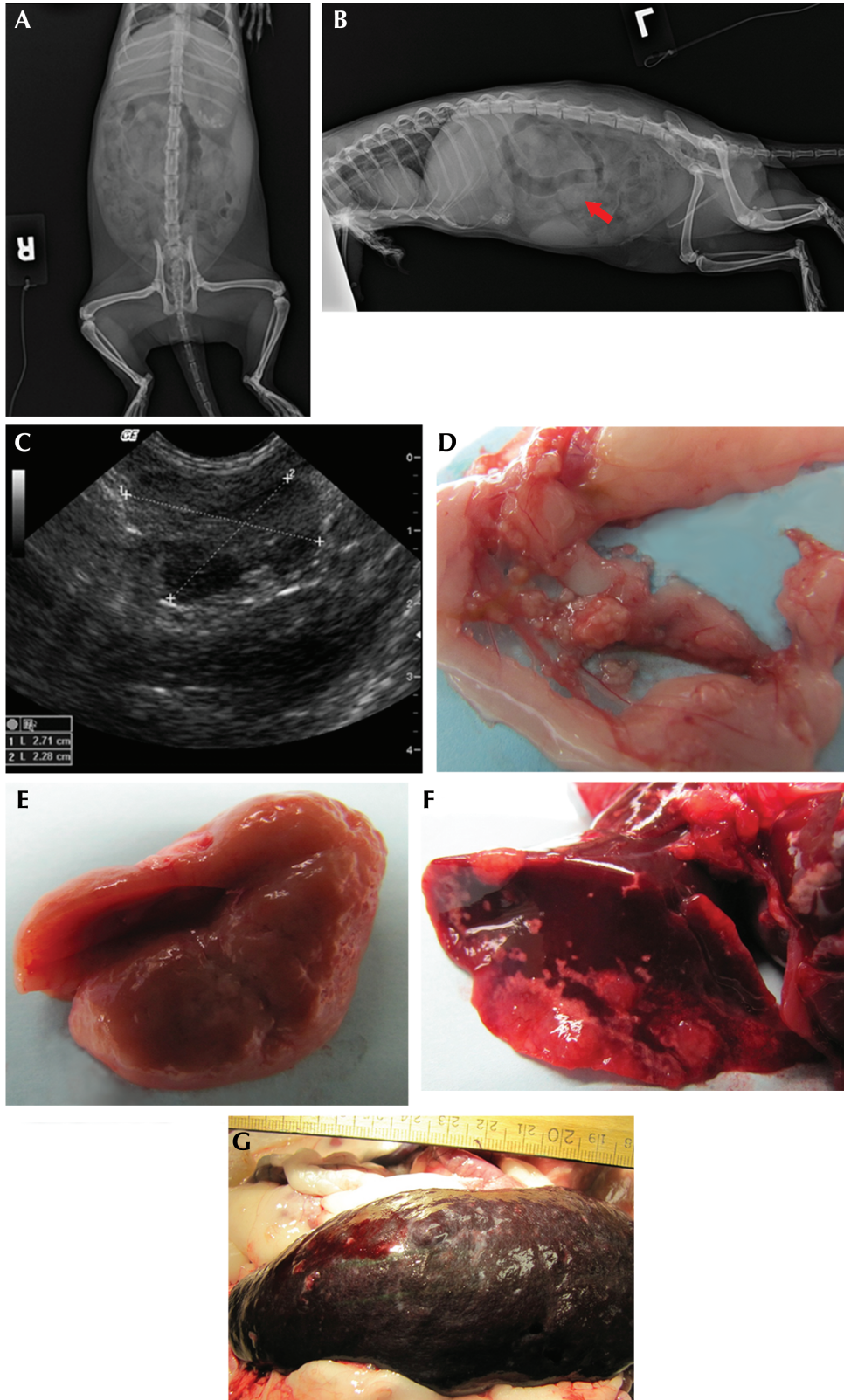


Figure 3. Case 3. (A) Ventrodorsal and (B) left lateral radiographs. Radiopaque foreign material is present in both views. The lateral view shows a poorly defined midabdominal area of increased density (arrow). (C) Ultrasonographic image of the midabdominal mass 5 wk after abdominal exploratory. (D) Multiple, firm, tan, 1- to 5-mm nodules throughout the mesentery. (E) Pitting lesions on kidney. (F) Multifocal, coalescing, raised white nodules on the lungs. (G) Enlarged spleen with multifocal pitting lesions.

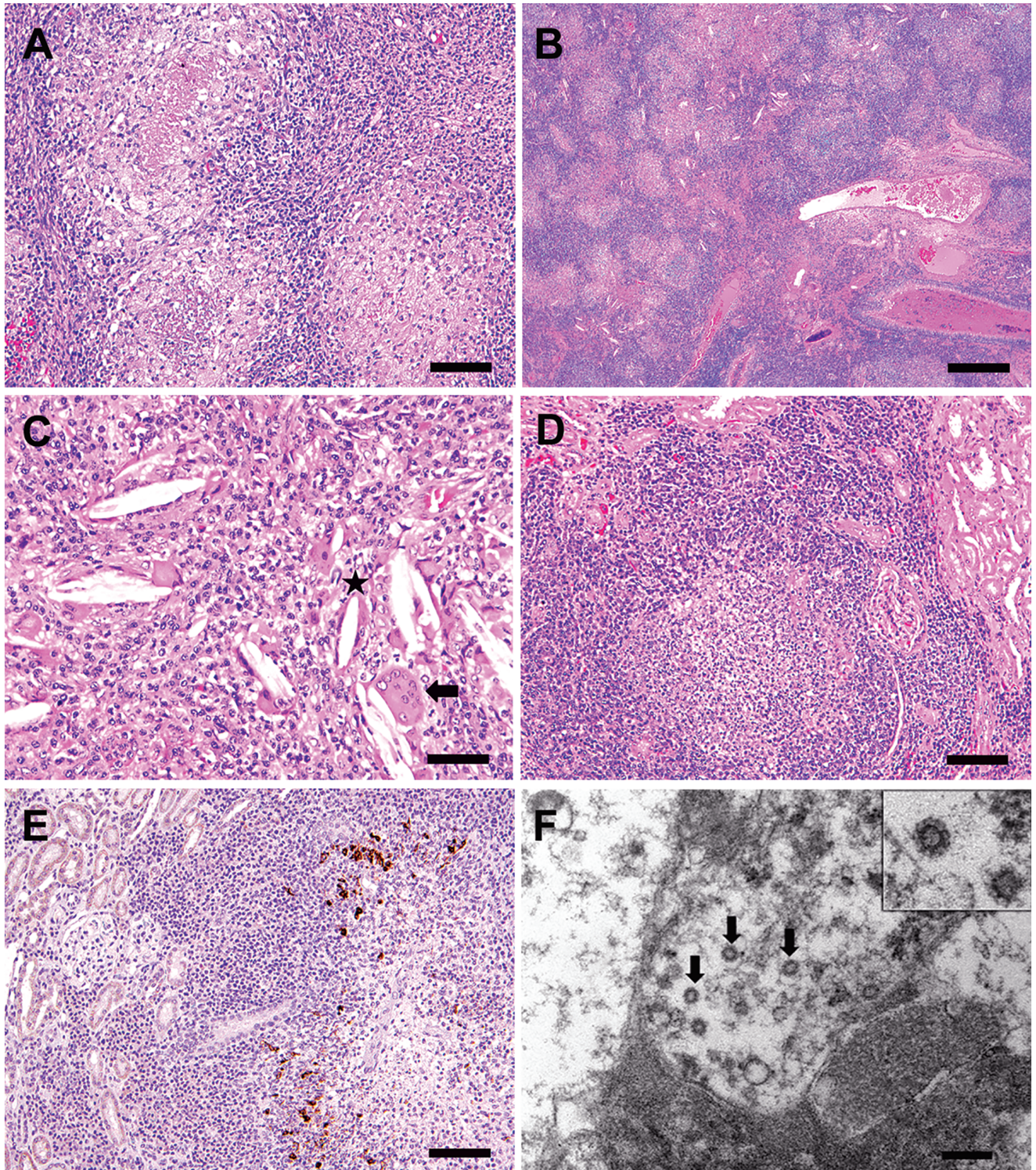


Figure 4. Case 3. (A) Multifocal to coalescing pyogranulomatous and lymphoplasmacytic lymphadenitis and peritonitis, with histologic features of central necrotic cores surrounded by neutrophils, macrophages and lymphocytes (bar, 100 μ M). (B) Severe granulomatous and lymphoplasmacytic pneumonia, with pulmonary architectural effacement and consolidation. Discernable bronchial and bronchiolar lumens are filled with eosinophilic proteinaceous material, mucus, and epithelial and inflammatory cellular debris (bar, 500 μ M). (C) Needle-like acicular cholesterol clefts (*) that are often associated closely with multinucleated giant cells (arrow; bar, 50 μ M). (D) Cortical lymphoplasmacytic interstitial nephritis (bar, 100 μ M). Hematoxylin and eosin stain (A through D) (E) Positive staining for feline coronavirus (FIPV3-70) monoclonal antibody within macrophages in granulomatous foci in the kidney, whereas plasma cells and lymphocytes in the interstitium are negative (bar, 100 μ M). (F) Electron microscopy of one of the mesenteric nodules reveals intracellular coronavirus-like particles (arrows). Virions were present in several nodules selected for examination and were found both within vacuoles and free in cytoplasm. Inset shows higher resolution image of a viral particle with the characteristic radiating crown-like coronavirus morphology (bar, 200 nM).

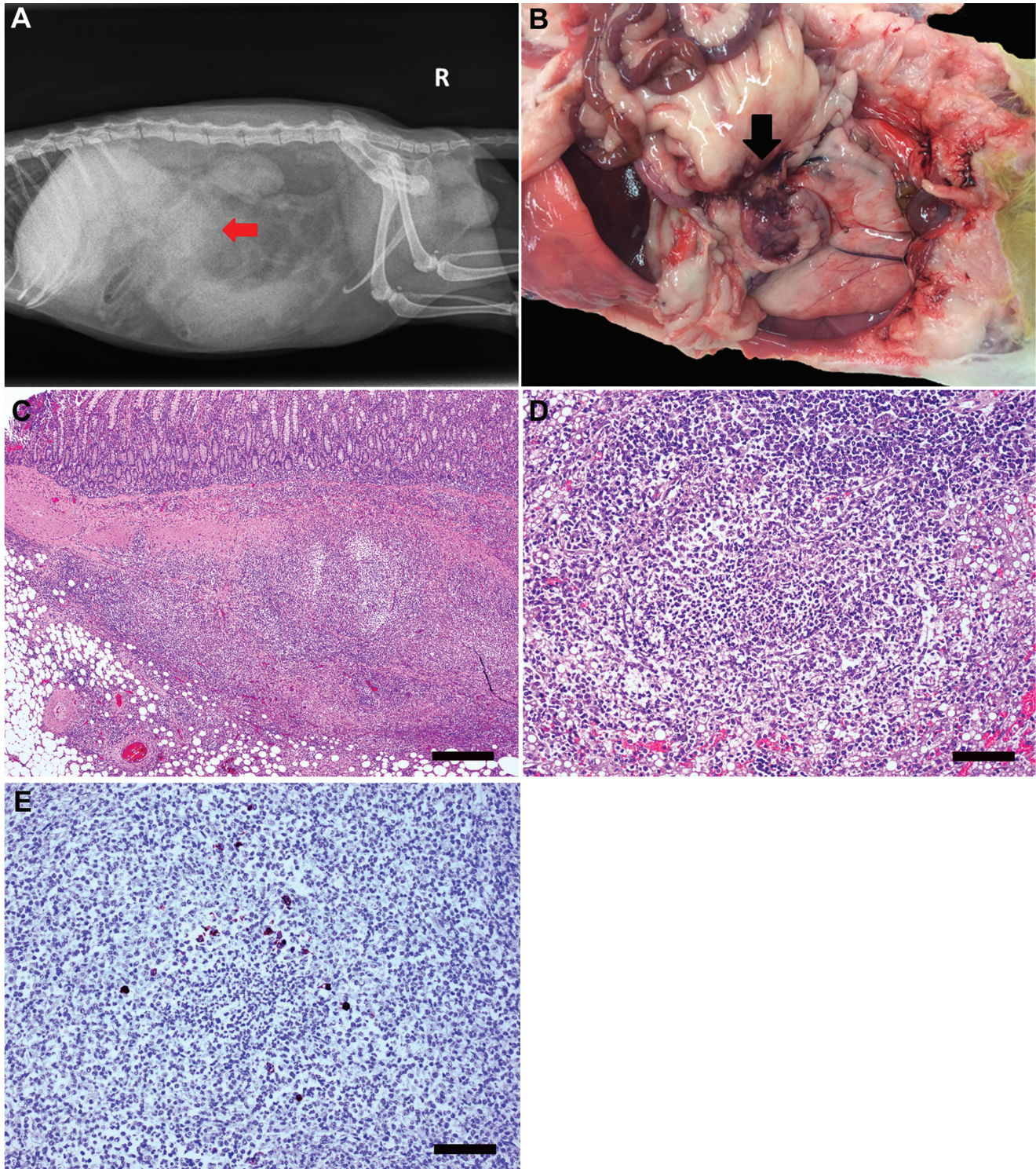


Figure 5. Case 5. (A) Right lateral radiograph depicting splenomegaly, decreased serosal detail, and an area of increased opacity (arrow) in the cranial midabdomen. (B) Nodular mesenteric mass firmly adhered to the small intestine (arrow). (C) Pyogranulomatous inflammation disrupts and effaces mesentery and small intestine. Hematoxylin and eosin stain; bar, 500 μ m. (D) Pyogranulomatous inflammation disrupts hepatic architecture. Inflammation is composed of minimal number of degenerate neutrophils surrounded by moderate numbers of epithelioid macrophages, lymphocytes, plasma cells, and fewer fibroblasts. Hepatocytes adjacent to the affected area have intracytoplasmic vacuoles (lipid type). Hematoxylin and eosin stain; bar, 100 μ m. (E) Epithelioid macrophages surrounding core neutrophils of a pyogranulomatous focus reveal strong intracytoplasmic immunoreactivity to feline coronavirus (FIPV3-70) monoclonal antibody (bar, 100 μ m).

using the FIPV3-70 monoclonal antibody was positive in lesions from the mesenteric root and lymph nodes.

Case 5. An adult, male, laboratory-housed ferret, approximately 1 y old, presented with clinical signs of intermittent depression, lethargy, inappetence, and 100-g weight loss over 4.5 mo. A markedly enlarged spleen and a midabdominal mass were palpable on physical exam. The ferret was housed alone in a modified rabbit cage within a room that contained several other individually housed ferrets. Serum biochemistry revealed hypoglycemia (74 mg/dL; reference range, 80 to 120 mg/dL), hyperglobulinemia (4.8 g/dL; reference, 0.2 to 2.4 g/dL), hypoalbuminemia (2.0 g/dL; reference, 3.4 to 4.8 g/dL), hypocalcemia (6.5 mg/dL; reference, 7.6 to 9.6 mg/dL), decreased BUN (9 mg/dL; reference, 10 to 45 mg/dL), hypercholesterolemia (273 mg/dL; reference, 96 to 249 mg/dL). Abdominal radiographs revealed splenomegaly and an area of increased opacity in the cranial midabdomen (Figure 5 A).

Gross postmortem findings included splenomegaly and a focal, irregular, 5 cm × 4 cm, tan, nodular mesenteric mass firmly adhered to the small intestine (Figure 5 B). In addition, the liver contained variably sized, slightly raised, tan foci. Histologically, the architecture of the mesentery, mesenteric lymph node, small intestine, and liver was disrupted and effaced by moderate multifocal to coalescing pyogranulomatous inflammation (Figure 5 C and D). The pyogranulomatous inflammation was characterized by a necrotic core composed of cellular and karyorrhectic debris admixed with degenerate neutrophils. The necrotic core was surrounded by an inner zone of epithelioid macrophages and an outer zone of lymphocytes, plasma cells, and few fibroblasts (Figure 5 D). The blood and lymphatic vessels in the mesentery and lymph node were ectatic and contained moderate amounts of eosinophilic material. The hepatic periportal interstitium and the perivascular interstitium of the mesentery were surrounded by low to moderate numbers of lymphocytes, plasma cells, and macrophages. Immunohistochemistry using FIPV3-70 monoclonal antibody revealed moderate intracytoplasmic immunoreactivity in macrophages that surrounded the necrotic core and degenerate neutrophils (Figure 5 E).

Discussion

Here we describe 5 confirmed cases of a systemic coronavirus-associated disease in ferrets that closely resembled the noneffusive, granulomatous form of feline infectious peritonitis in cats. These cases originated from multiple sources, including private veterinary practice and a laboratory animal facility at an accredited institution. This disease initially was reported in the literature in Spain^{5,6} and subsequently diagnosed in ferrets from the United States,² New Zealand, Netherlands,¹⁰ Japan,⁷ and the United Kingdom.³ However, the earliest report of a disease process in ferrets with strikingly similar clinical signs and pathologic findings to FRSCV was in Denmark in 1951, where the authors classified the disease as an enzootic malignant granulomatosis of unknown etiology.⁸ The early case series described 142 ferrets, the majority of which were younger than 1 y, with clinical signs of progressive anorexia and weight loss with palpable abdominal masses. Histologically, granulomatous inflammatory changes were most commonly seen in the mesenteric lymph nodes, spleen, and liver; lacked bacteria, fungal hyphae, and protozoa; and yielded negative aerobic, anaerobic, and mycobacterial cultures.⁸

Differential diagnoses for the 5 cases we presented include mycobacteriosis and systemic fungal infections, but no acid-fast

bacilli or fungal organisms were identified. In addition, the distribution and nature of the lesions mimic those seen with chronic Aleutian disease, a highly contagious parvovirus seen in minks and ferrets.¹ Typical clinicopathologic findings in Aleutian disease include progressive wasting and weight loss, splenomegaly, hypergammaglobulinemia, chronic glomerulonephritis, lymphoplasmacytic interstitial nephritis, and prominent arteritis involving kidneys and other organs. Definitive diagnosis of Aleutian disease is based on PCR-based testing or in situ hybridization to demonstrate viral antigen or antibodies within lymphoplasmacytic infiltrates with concurrent hypergammaglobulinemia. Because the 5 ferrets we present were not tested, Aleutian disease cannot be completely ruled out as a concomitant infection. However, hyperglobulinemia was seen in only 1 of the 5 ferrets and positive immunoreactivity to FIPV3-70 antibody seen in all 5 animals, thus making a diagnosis of Aleutian disease unlikely. Myofasciitis can have a similar clinical presentation but is not histologically comparable to Aleutian disease or FRSCV.¹

As is the case for feline infectious peritonitis and has been documented in the previous reports of FRSCV-associated disease, these diseases have no definitive treatment.^{4,9} Immunosuppressive therapy and symptomatic and supportive care including nutritional and vitamin supplementation, gastroprotectants, antiemetics, and empirical antibiotic therapy are currently the recommended interventions and were helpful in maintaining a favorable quality of life for 1 y after diagnosis in one of the ferrets we describe. The route for transmission of the FRSCV-associated disease is unknown but is suggested to be fecal–oral, similar to that for FCoV; therefore measures aimed toward preventing the spread of the disease, particularly where multiple ferrets cohabitate, should be adapted from recommendations for the prevention of feline infectious peritonitis in cats.⁴ Feline coronaviruses typically infect domestic and exotic felids and are classified into 2 serotypes according to their genetic sequence. Type I FCoV are unique to felines and are more common worldwide than are type II FCoV, which are the result of recombination between type I FCoV and canine coronavirus. Both types have been shown to cause FIP, and cats can exhibit simultaneous coinfections. Although FCoV, ferret enteric coronavirus, and FRSCV are all classified as group 1 coronaviruses (that is, alphacoronaviruses) along with other enteric diseases of domestic animals including transmissible gastroenteritis of swine and canine coronavirus, FCoV is genetically distinct from the ferret coronaviruses. With the increasing prevalence of publications reporting the diagnosis of FRSCV in the literature, it is important to consider this viral disease as a differential diagnosis for young, debilitated ferrets with abdominal masses.

Acknowledgment

This study was supported by NIH grants T32-OD010978-26 and P30-ES002109 (both to JGF).

References

1. Fox JG, Marini RP, editors. 2014. *Biology and diseases of the ferret*, 3rd ed. Ames (IA): Wiley.
2. Garner MM, Ramsell K, Morera N, Juan-Salles C, Jimenez J, Ardiaca M, Montesinos A, Teifke JP, Lohr CV, Evermann JF, Baszler TV, Nordhausen RW, Wise AG, Maes RK, Kiupel M. 2008. Clinicopathologic features of a systemic coronavirus-associated disease resembling feline infectious peritonitis in the domestic ferret (*Mustela putorius*). *Vet Pathol* 45:236–246.

3. **Graham E, Lamm C, Denk D, Stidworthy MF, Carrasco DC, Kubiak M.** 2012. Systemic coronavirus-associated disease resembling feline infectious peritonitis in ferrets in the UK. *Vet Rec* **171**:200–201.
4. **Greene CE.** 2012. *Infectious diseases of the dog and cat*, 4th ed. St Louis (MO): Elsevier–Saunders.
5. **Martinez J, Ramis AJ, Reinacher M, Perpignan D.** 2006. Detection of feline infectious peritonitis virus-like antigen in ferrets. *Vet Rec* **158**:523.
6. **Martinez J, Reinacher M, Perpignan D, Ramis A.** 2008. Identification of group 1 coronavirus antigen in multisystemic granulomatous lesions in ferrets (*Mustela putorius furo*). *J Comp Pathol* **138**:54–58.
7. **Michimae Y, Mikami S, Okimoto K, Toyosawa K, Matsumoto I, Kouchi M, Koujitani T, Inoue T, Seki T.** 2010. The first case of feline infectious peritonitis-like pyogranuloma in a ferret infected by coronavirus in Japan. *J Toxicol Pathol* **23**:99–101.
8. **Momberg-Jorgensen HC.** 1951. Enzootic malignant granulomatosis in ferrets. *Acta Pathol Microbiol Scand* **29**:297–306.
9. **Murray J, Kiupel M, Maes RK.** 2010. Ferret coronavirus-associated diseases. *Vet Clin North Am Exot Anim Pract* **13**:543–560.
10. **Perpignan D, Lopez C.** 2008. Clinical aspects of systemic granulomatous inflammatory syndrome in ferrets (*Mustela putorius furo*). *Vet Rec* **162**:180–183.
11. **Williams BH, Kiupel M, West KH, Raymond JT, Grant CK, Glickman LT.** 2000. Coronavirus-associated epizootic catarrhal enteritis in ferrets. *J Am Vet Med Assoc* **217**:526–530.